

Steps, Hops and Turns: Examining the effects of Channel Shapes on Mass transfer in Continuous Electrochemical Reactors

Hamish R. Stephen,^a Sarah Boyall,^a Christiane Schotten,^a Thomas P. Nicholls,^a Richard A. Bourne,^b Nikil Kapur,^{*c} and Charlotte E. Willans^{*a}

^a School of Chemistry, University of Leeds, Leeds LS2 9JT, UK.

^b Institute of Process Research and Development, School of Chemistry & School of Chemical and Process Engineering, University of Leeds, Leeds LS2 9JT, UK.

^c School of Mechanical Engineering, University of Leeds, Leeds LS2 9JT, UK.

Supplementary information

Contents

1. General considerations	3
2. Third generation reactor	4
2.1. Reactor manufacture and assembly	4
2.2. Spacer design	6
3. Copper-NHC reaction	7
3.1. General procedure for the synthesis of Cu1	7
3.2. Testing different spacers	8
4. Computational Fluid Dynamics Study of Mass Transport from electrode surface	11
4.1. Modelling fluid flow	11
4.2. Simulating material transport from the electrode	12
4.3. Flow channel designs.....	13
4.3.1. Straight channel	13
4.3.2. Channel with turns	16
4.3.3. Channel with hops.....	18
4.3.4. Channel with stepped turns	20

5. Systematic study	22
5.1. Reactor and spacer design.....	22
5.2. Reactor characterisation	23
5.2.1. Residence time distributions.....	23
5.2.2. Mass transfer coefficients.....	24
6. References	32

1. General considerations

NMR data were obtained on either a Bruker AVNeo 500 (CH dual cryoprobe) or Bruker Ascend 400 spectrometer. ^1H NMR and $^{13}\text{C}\{^1\text{H}\}$ chemical shifts were referenced against residual solvent peaks. Mass spectra were collected on a Bruker Daltonics (micro TOF) instrument operating in the electrospray mode. Elemental Analyses were performed by Mr Stephen Boyer at London Metropolitan University.

Unless otherwise noted all reagents employed in these studies were used as received from Sigma-Aldrich, Fluorochem, Fischer Scientific or Acros Organics and used without purification. Anhydrous solvents were dried by passing over activated alumina to remove water, copper catalyst to remove oxygen, and molecular sieves to remove any remaining water, *via* the Dow-Grubbs solvent system. Toluene, and DCM were freeze-pump-thaw degassed, while other solvents were degassed by purging with argon.

2. Third generation reactor

2.1. Reactor manufacture and assembly

The third generation electrochemical flow reactor was machined from stainless steel by the workshop in the School of Mechanical Engineering at the University of Leeds. Electrodes and spacers were designed on Corel Draw. Copper electrodes were laser cut by Laser Master (Redruth, TR16 6HY) from C160 copper sheet with a thickness of 0.9 mm. Spacers were laser cut by Laser Web (Barnsley, S71 3HS) from PTFE sheets with a thickness of 1 mm.

The third generation reactor features stacked electrodes which alternate between cathode and anode with PTFE spacers in between (Figure S1). PTFE gaskets insulate the stainless steel housing and M5 bolts are used to sandwich the reactor together. The volume can be varied by changing the number of PTFE spacers that are used, with one A spacer giving a volume of approximately 0.5 mL.

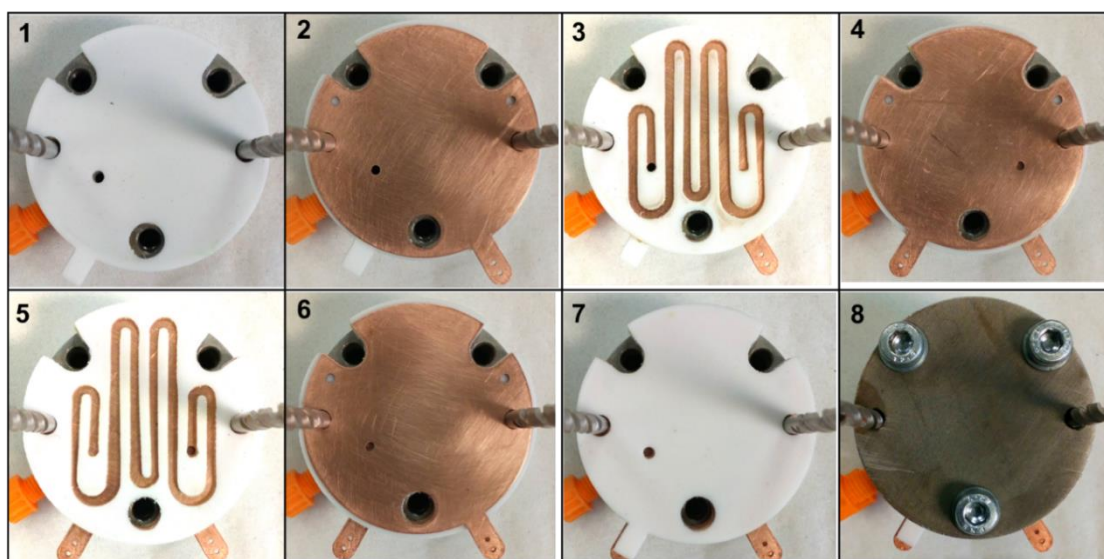


Figure S1: Assembling the third generation reactor: insulating PTFE gasket (1), electrode (2), spacer (3), electrode (4), spacer (5), electrode (6), gasket (7) and the steel housing (8).

Where multiple spacers are used the solution must pass through an electrode in what we refer to as a hop (Figure S2).

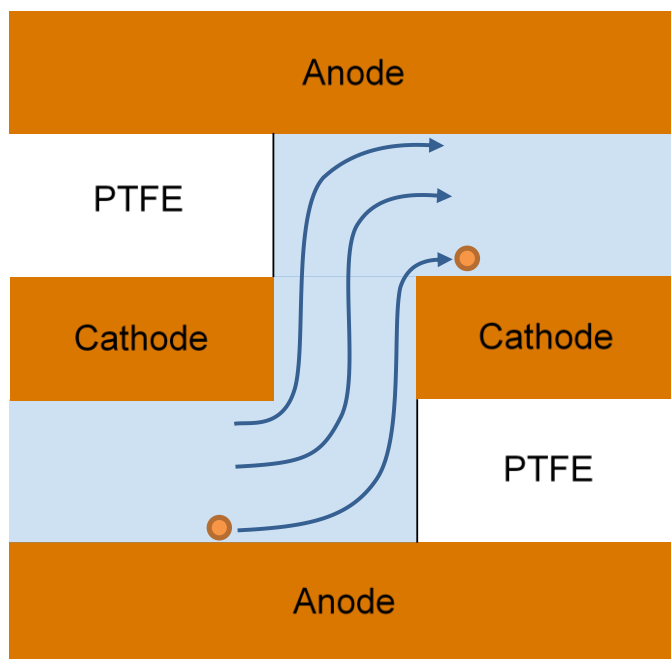
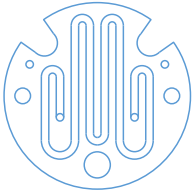
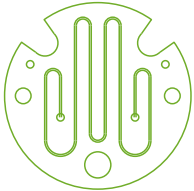
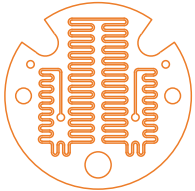
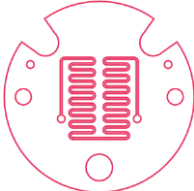
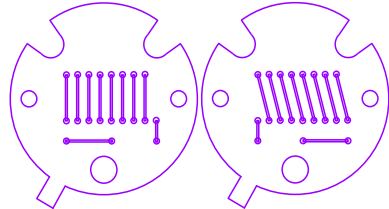


Figure S2: Representation of a hop in the flow channel.

2.2. Spacer design

Five spacers (**A-E**) were designed with a thickness of 1 mm, whilst the width and number of turns in each spacer was varied. Volumes were calculated from the area of the flow channels.

Spacer	A	B	C	D	E
					
Channel width	2 mm	0.5 mm	0.5 mm	0.5 mm	0.5 mm
Number of turns	7	7	82	30	0
Volume	0.463 mL	0.128 mL	0.260 mL	0.128 mL	0.162 (pair)
Number of spacers to get 0.5 mL	1	4	2	4	3 pairs
Turns per 0.5 mL	7	28	164	120	0
Hops per 0.5 mL	0	3	1	3	60

3. Copper-NHC reaction

3.1. General procedure for the synthesis of Cu1

The electrochemical synthesis of Cu(IMes)Cl (**Cu1**) from IMesHCl (**L1**) is a well-established reaction that has previously been used by our group as a model reaction.^{1,2} **L1** was prepared *via* literature procedures.³ 6mM solutions of **L1** in anhydrous acetonitrile were prepared under argon. The solution was transferred to a syringe and pumped through the reactor using a syringe pump. A constant potential of 1.8 V was applied using a Tenma bench top power supply (72-10480 from Farnell) with a multimeter and alternating polarity microcontroller (Arduino MKZERO with Arduino MKR relay proto shield) set to 1/60 Hz in series (Figure S3).²

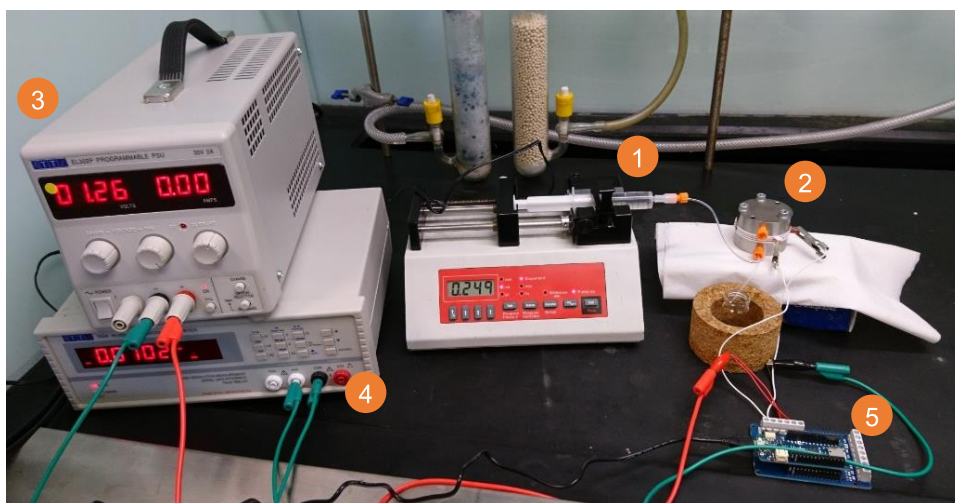
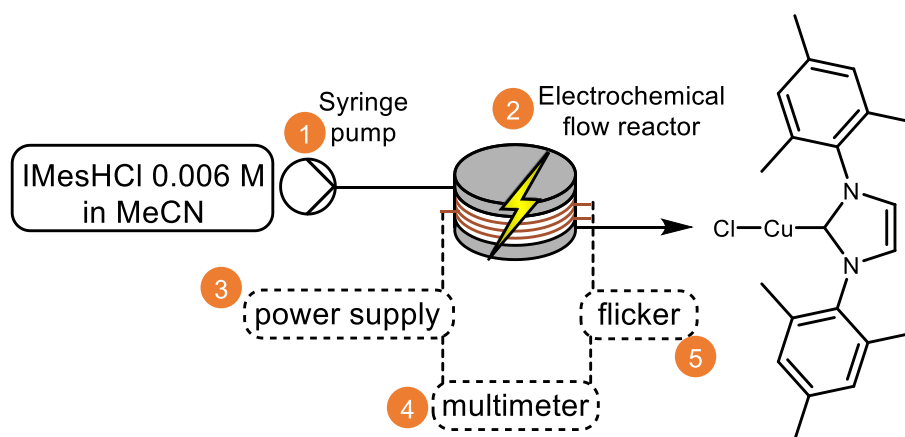


Figure S3: Set up of the electrochemical flow reactor.

Two residence times were allowed to elapse for the reactor to reach steady state (Table S1), before the eluent was collected for one residence time in a round bottomed flask in air. The solvent was removed under vacuum and the remaining white solid dissolved in

deuterated chloroform. ^1H NMR spectroscopy was used to calculate the conversion from the integrals of the imidazolium salt and the copper-NHC complex at δ 7.59 ppm (s, 2H, $\text{Imid}_{\text{backbone}}$) and 7.00 ppm (s, 4H, ArH) respectively (Table S2).

\dot{V} / mL min $^{-1}$	τ / min	Wait time / min	Collection time / min
0.04	12.50	25	10
0.08	6.25	15	5
0.12	4.17	10	4
0.16	3.13	8	3
0.20	2.50	6	2

Table S1: Residence times, time to reach steady state and the collection times when the volume of the reactor is 0.5 mL.

Proton	L1 (ppm)	Cu1 (ppm)
NCHN	10.89	-
$\text{Imid}_{\text{backbone}}$	7.59	7.05
ArH	7.03	7.00
<i>p</i> -CH $_3$	2.18	2.34
<i>o</i> -CH $_3$	2.34	2.10

Table S2: Chemical shifts for L1 and Cu1.

In between each reaction the reactor was disassembled and the electrodes cleaned. The copper electrodes were cleaned by rinsing with acetone, sandpapering, washing with HCl (~3 M) and rinsed a second time with acetone.

3.2. Testing different spacers

The general electrochemical flow procedure was followed, using different spacers each with a volume of approximately 0.5 mL at a range of flow rates. Numerous experiments were conducted using different batches of L1 and anhydrous acetonitrile. Each reaction was performed a minimum of two times and a mean of the conversion at each flow rate was calculated for each spacer. This was plotted against the residence time and the standard error calculated for each point.

A (1 spacer)					
Residence time	11.58	5.79	3.86	2.89	2.32
Conversion	97.3	69.2	61.7	49.2	41.3
	88.9	70.3	61.5	51.9	51.3
	97.1	76.5	56.0	60.9	52.3

	96.8	74.5	64.5	60.2	57.3
	81.2		63.2		
	85.6		65.9		
			67.0		
			65.2		
			83.6		
			81.6		
			62.3		
Mean	91.1	72.6	66.6	55.5	50.6
SD	6.3	3.0	8.0	5.1	5.8
Standard error	2.6	1.5	2.4	2.5	2.9

Table S3: Combined data for **A**. Volume = 0.463 mL.

B (4 spacers)					
Residence time	12.80	6.40	4.27	3.20	2.56
Conversion	100.0	82.2	69.2	75.2	68.9
	94.2	80.8	67.0	68.7	59.8
		79.3	76.1	65.8	58.4
			71.6		
Mean	97.1	80.7	71.0	69.9	62.4
SD	2.9	1.2	3.4	3.9	4.7
Standard error	2.0	0.7	1.7	2.3	2.7

Table S4: Combined data for **B**. Volume = 0.512 mL.

C (2 spacers)					
Residence time	13.00	6.50	4.33	3.25	2.60
Conversion	96.7	81.0	68.3	60.6	61.0
	97.2	91.1	78.3	74.4	66.0
	97.6	82.3	73.0	69.7	75.7
	99.1	91.7	69.9		65.4
		81.7	75.8		70.8
			79.6		

Mean	97.6	85.5	74.1	68.3	67.8
SD	0.9	4.8	4.1	5.7	5.0
Standard error	0.4	2.1	1.7	3.3	2.2

Table S5: Combined data for **C**. Volume = 0.520 mL.

D (4 spacers)					
Residence time	12.80	6.40	4.27	3.20	2.56
Conversion	98.6	83.7	74.1	73.8	66.0
	99.4	92.8	74.1	70.2	72.1
		85.3	80.4		70.7
			77.3		
Mean	99.0	87.3	76.5	72.0	69.6
SD	0.4	4.0	2.6	1.8	2.6
Standard error	0.3	2.3	1.3	1.3	1.5

Table S6: Combined data for **D**. Volume = 0.512 mL.

E (3 pairs of spacers)					
Residence time	12.15	6.08	4.05	3.04	2.43
Conversion	100.0	94.7	82.5	60.7	57.6
	100.0	88.2	80.4	74.6	58.2
	100.0	88.9	76.6	75.0	71.0
Mean	100.0	90.6	79.8	70.1	62.3
SD	0.0	2.9	2.5	6.6	6.2
Standard error	0.0	1.7	1.4	3.8	3.6

Table S7: Combined data for **E**. Volume = 0.486 mL.

4. Computational Fluid Dynamics Study of Mass Transport from electrode surface.

Computational fluid dynamics (CFD) were conducted using the laminar flow and transport of diluted species packages within Comsol Multiphysics 5.5. This uses the finite element method⁴ to solve the Navier Stokes equations (for flow) and the advection-diffusion equation for modelling the transport of species within the electrochemical reactor. The steps in this are (i) define a geometry; (ii) assign inlet, outlet and wall boundary conditions; (iii) solve the steady state flow field; (iv) define the inlet concentration and wall concentration; (v) solve the advection-diffusion equation with the flow field being defined by step iii; (vi) calculate the mean concentration at positions down the channel; (vii) rank the mass transport from the channel wall to the bulk flow as a function of geometry.

The approach where one surface is held at a concentration of 1 (with the others at 0) does not explicitly model the electrochemical process, but it does capture the transport of material away from the electrode surface under the limit of mass transport. This allows comparative evaluation of the mass transfer characteristics of the flow cell design, whilst considerably simplifying the modelling process, when compared to a full kinetic model.

Throughout the simulation the reference pressure and temperature were set to 1 atmosphere and 293.15 K respectively. The fluid was modelled as water with a density of 997 kg m⁻³ and a viscosity of 0.001 Pa S. The species had diffusion coefficients of 1x10⁻⁹ m² s⁻¹.

4.1. Modelling fluid flow

The velocity fields were modelled using the laminar flow equations for a steady state flow. using the Navier-Stokes equation and conservation of mass:

$$\rho(u \cdot \nabla)u = \nabla P + \mu \nabla \cdot [\nabla u + \nabla u^T] + F$$

$$\rho \nabla \cdot u = 0$$

Equation S1: Navier-Stokes equation. Where ρ is the density, u is the velocity field, μ the viscosity, P is the pressure, F is the volume force vector (body force in this case).

The inlet boundary was set to a velocity of 0.001 m s⁻¹ with a flat inflow velocity. The outlet was set to suppress backflow and the remaining walls had a no-slip boundary condition applied to them. The pressure drop was calculated for each of the flow channels.

Channel	P inlet / Pa	P outlet / Pa	P drop / Pa
Straight	2.8256	0.0026	2.8230
Turns	2.8605	0.0030	2.8575
Steps	3.1301	0.0028	3.1273
Hops	3.1295	0.0028	3.1267

Table S8: Pressure drop for the four flow channels.

4.2. Simulating material transport from the electrode

The transport of dilute species package within Comsol was used to simulate the flux of a chemical species leaving the surface of an electrode. To do this, one wall of the channel was set to a concentration of 1 mol m^{-3} (shown as a blue surface in Figures S7, S10, S13 and S14) with the inlet concentration of fluid set to 0 mol m^{-3} . The remaining boundaries, apart from the outlet, were set to have no flux transport across them.

The transport of material away from this electrode into the bulk is as a result of advection (with the flow field calculated using equation S1) and diffusion with equation S2, the advection-diffusion equation is used to calculate the movement of the solute.

$$\nabla \cdot J_i + u \cdot \nabla c_i = R_i$$

$$J_i = -D_i \nabla c_i$$

Equation S2: Calculating the concentration. Where J_i is the mass flux diffusive flux vector, u is the flow velocity vector, c_i is the concentration of the species, R_i is the reaction rate expression – here zero- and D_i is the diffusion coefficient.

The concentration was then reported as an average concentration from a series of planes taken normal to the flow at positions down the channel (Figure S4). The mean concentration captures the mass transfer away from this surface, with the flow parameters and channel geometry influencing this rate.

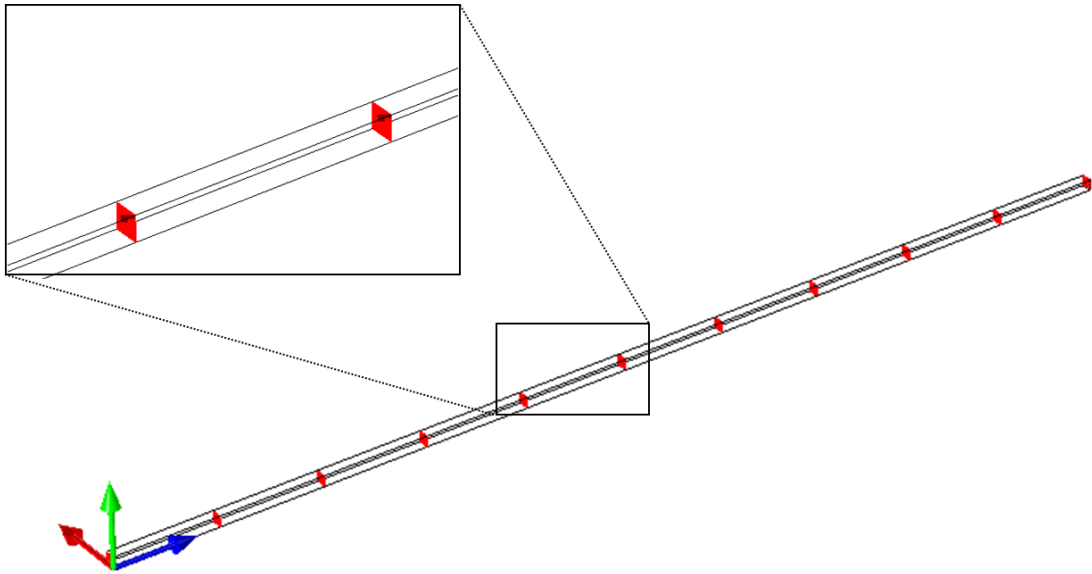


Figure S4: Planes across the channels were used to calculate the mean concentration at intervals along the channel.

4.3. Flow channel designs

Four flow channels were modelled. All had a depth and width of 1 mm. The fluid properties were taken as water at 25°C. Once constructed the mesh was generated using physics-controlled mesh with the element size set to normal.

4.3.1. Straight channel

The straight channel was a simple cuboid 1 mm x 1 mm x 100 mm. 495368 elements were used to construct the mesh.

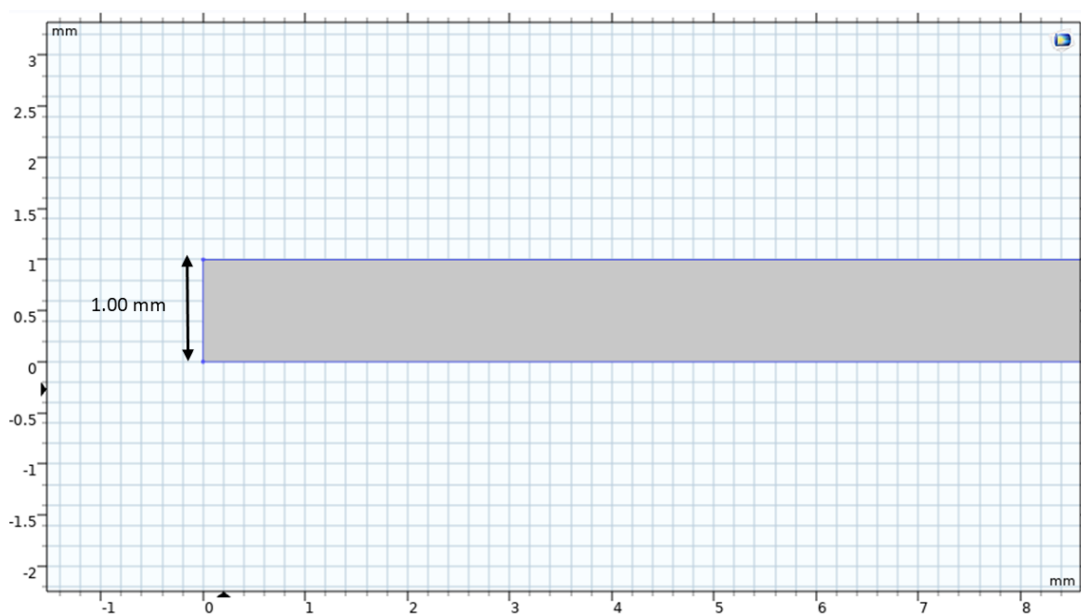


Figure S5: Dimensions of the straight channel.

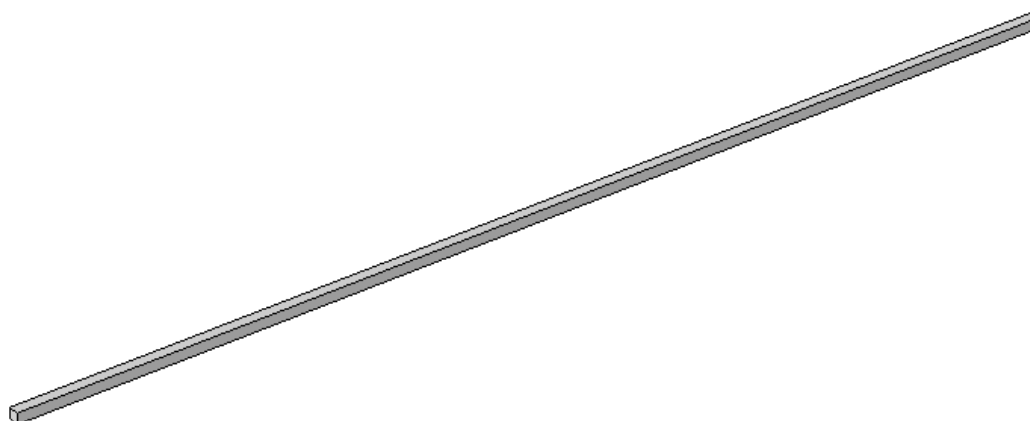
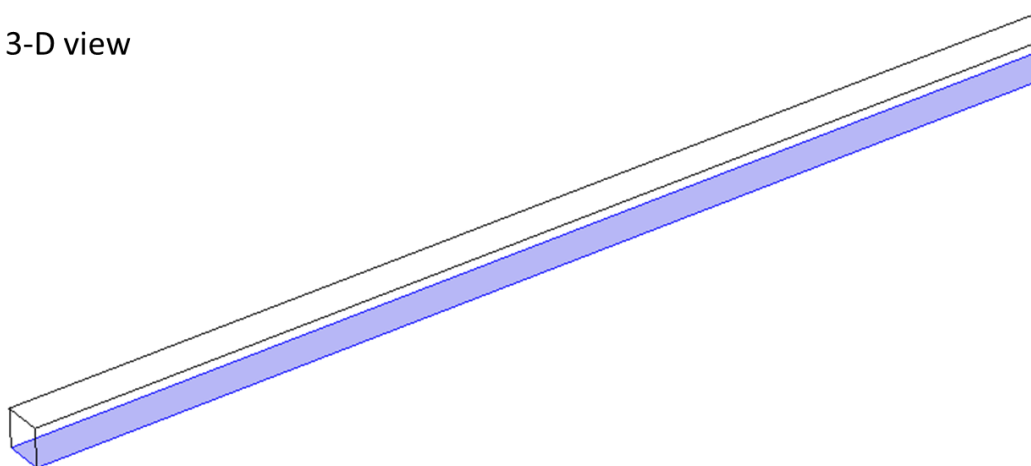


Figure S6: Straight channel used in the CFD studies.

The bottom wall of the straight channel was used to act as the electrode (shown in blue).

a) 3-D view



b) Top view



Figure S7: Position of the electrode in the straight channel.

Height / mm	1
Width / mm	1
Length / mm	100
Electrode area / mm ²	100
Volume / mm ³	100

Table S9: Dimensions of the straight channel.

Distance / mm	Mean concentration / mol m ⁻³
0	0.007
10	0.148
20	0.206
30	0.257
40	0.302
50	0.344
60	0.382
70	0.419
80	0.453
90	0.484
100	0.510

Table S10: Mean concentrations at distances along the straight channel.

4.3.2. Channel with turns

The channel with turns was constructed in a 2D plane from 10 repeating units, with a channel width of 1 mm and centre-line path length of 100 mm. This was extruded by 1 mm in the z-direction (out of the page) to give a flow channel with square cross section (1 mm by 1 mm). 303356 elements were used to construct the mesh.

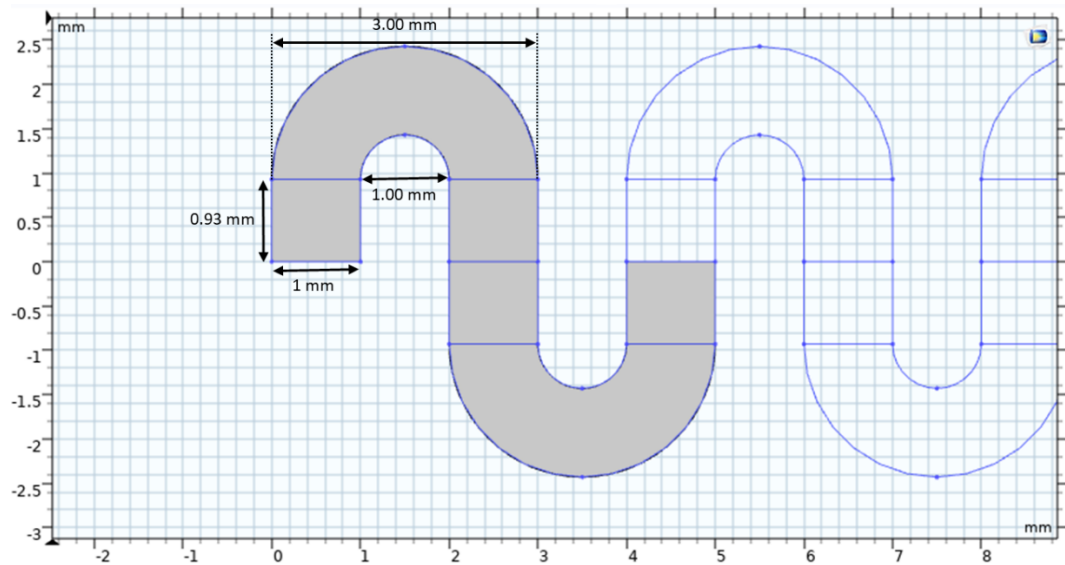


Figure S8: Dimensions of the turns used to construct the channel with turns.

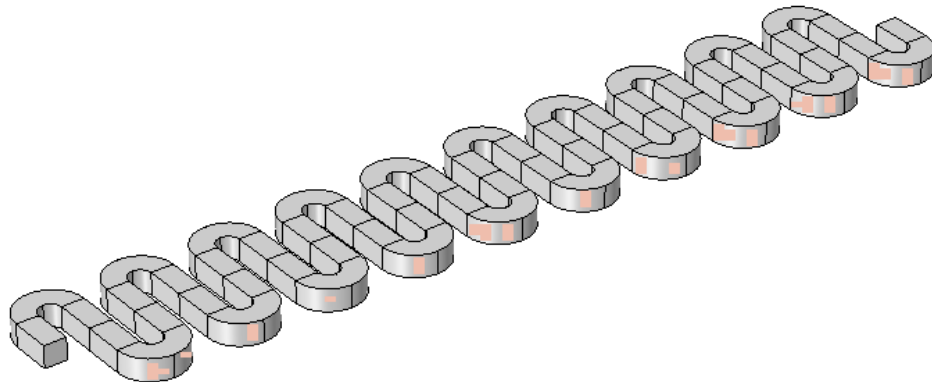
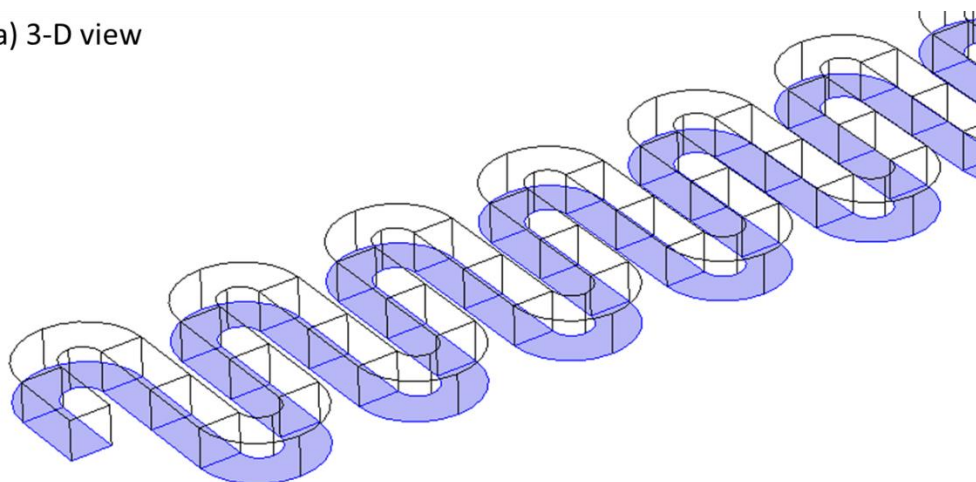


Figure S9: Channel with turns.

The bottom wall of the channel with turns was used to act as the electrode (shown in blue).

a) 3-D view



b) Top view

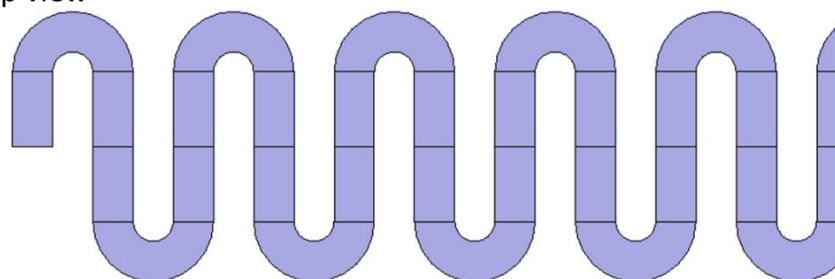


Figure S10: Position of the electrode in the channel with turns.

Height / mm	1
Width / mm	1
Length / mm	100
Electrode area / mm ²	100
Volume / mm ³	100

Table S11: Dimensions of the channel with turns.

Distance / mm	Mean concentration / mol m ⁻³
0	0.010
5	0.107
10	0.143
15	0.175
20	0.204
25	0.232
30	0.257
35	0.282
40	0.305
45	0.329
50	0.350
55	0.371

60	0.391
65	0.411
70	0.429
75	0.447
80	0.464
85	0.481
90	0.497
95	0.513
100	0.523

Table S12: Mean concentrations at distances along the channel with turns.

4.3.3. Channel with hops

The channel with turns was constructed in a 2D plane from 10 repeating units, with a channel width of 1 mm and centre-line path length of 120 mm. This was extruded by 1 mm to give a flow channel with square cross section (1 mm by 1 mm). 387120 elements were used to construct the mesh.

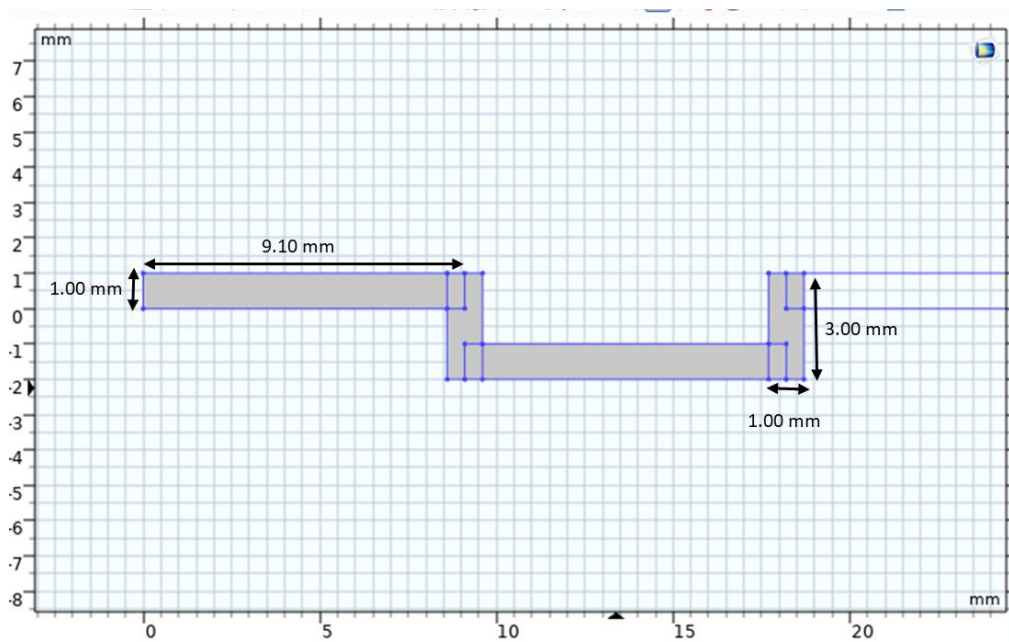


Figure S11: Dimensions of the 90° turns used to construct the channel with hops and the channel with stepped turns.

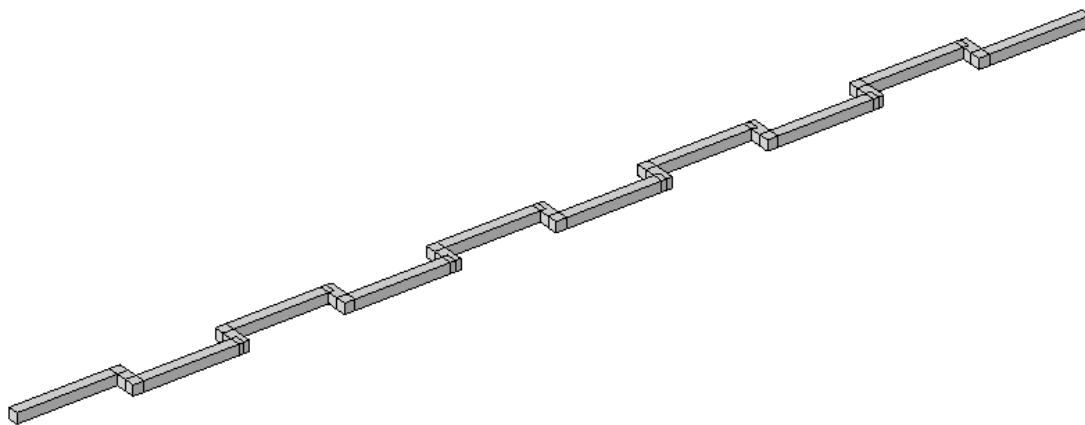
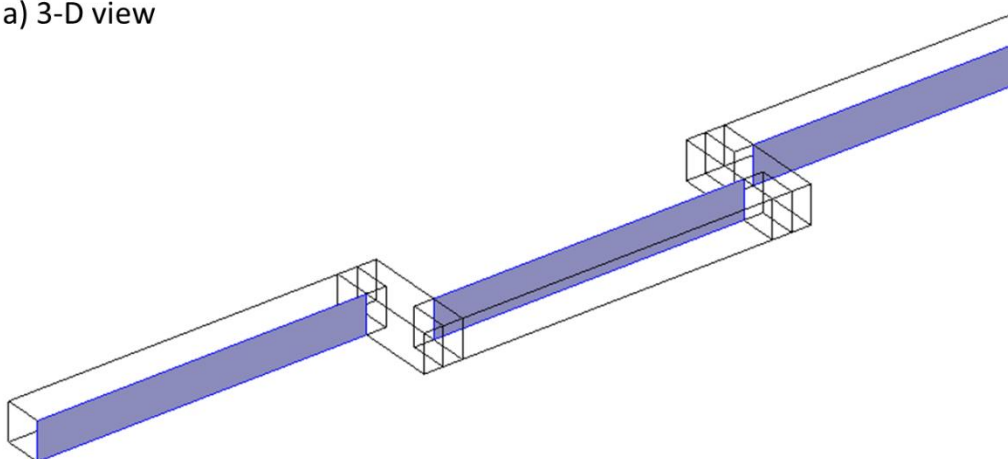


Figure S12: Channel with hops and channel with stepped turns.

The channel with hops had the electrode such that it alternated which side of the channel it was on every time the channel went through a dogleg.

a) 3-D view



b) Top view



Figure S13: Position of the electrode in the channel with hops.

Height / mm	1
Width / mm	1
Length / mm	120
Electrode area / mm ²	91
Volume / mm ³	120

Table S13: Dimensions of the channel with hops.

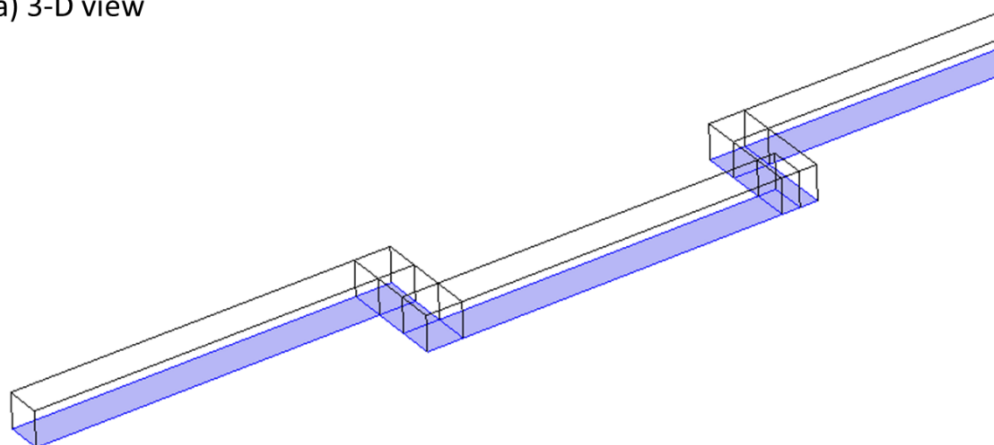
Distance / mm	Mean concentration / mol m ⁻³
0	0.014
4.3	0.106
15.4	0.209
26.5	0.291
37.6	0.366
48.7	0.432
59.8	0.493
70.9	0.547
82	0.594
93.1	0.637
104.2	0.675
115.3	0.709
120	0.716

Table S14: Mean concentrations at distances along the channel with hops.

4.3.4. Channel with stepped turns

The geometries of the channel with steps is the same as the one with hops, but the electrode remains on the same side of the channel. This was to distinguish between the shape of the channel with hops (i.e. 90° turns) with the position of the electrode.

a) 3-D view



b) Top view



Figure S14: Position of the electrode in the channel with stepped turns.

Height / mm	1
Width / mm	1
Length / mm	120
Electrode area / mm ²	120
Volume / mm ³	120

Table S15: Dimensions of the channel with steps.

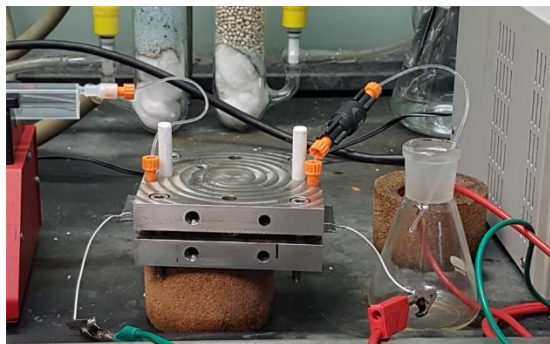
Distance / mm	Mean concentration / mol m ⁻³
0	0.015
4.3	0.105
15.4	0.182
26.5	0.246
37.6	0.300
48.7	0.350
59.8	0.398
70.9	0.442
82	0.481
93.1	0.519
104.2	0.552
115.3	0.584
120	0.592

Table S16: Mean concentrations at distances along the channel with steps.

5. Systematic study

5.1. Reactor and spacer design

One of our second-generation reactors¹ was adapted by the workshop in the School of Mechanical Engineering at the University of Leeds by machining two ¼-28 fittings 90 mm apart.



Graphite electrodes were cut from graphite foil purchased from Alfa Aesar (43083, 1 mm thick). Spacers were laser cut by Laser Web (Barnsley, S71 3HS) from PTFE sheets with a thickness of 1 mm. 4 spacers were designed so that they had width and depth of 1 mm. Each channel had a path length of 90 mm, giving a volume of 90 mm³. Volumes were calculated from the area of the flow channels using Coral Draw.

A straight channel (**F**) was included as a control. A channel with turns (**G**) was made to test the effect of adding turns. **H** was included to test the effect of 90° turns and to compare with the channel with hops. **H** and **I** have very similar geometries, the difference being that **H** remains within two electrodes, whilst **I** passes through an electrode in a series of hops.

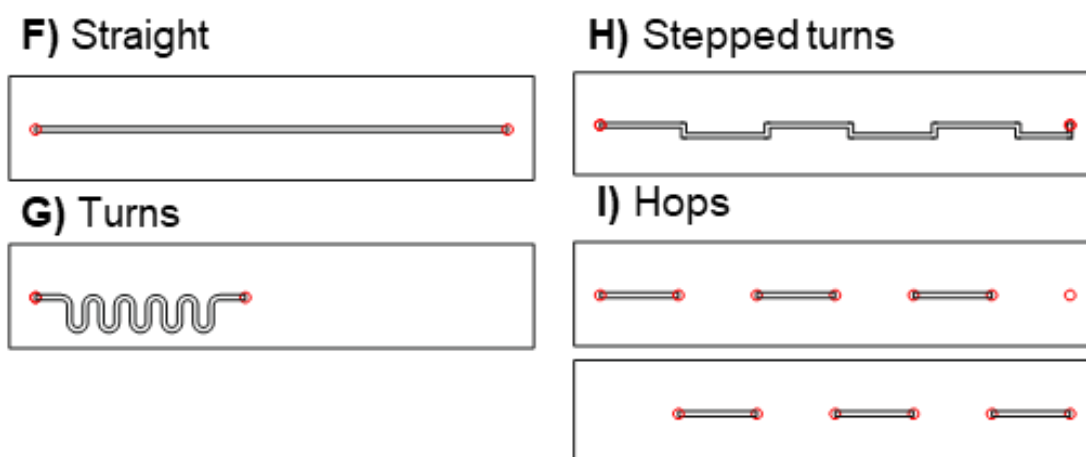


Figure S15: Flow channels used in the systematic study.

5.2. Reactor characterisation

5.2.1. Residence time distributions

A solution of methylene blue (20 mg, 0.063 mmol) in acetonitrile (100 mL) was pumped into a 15 μL sample loop and then pumped through the reactor with a solution of acetonitrile at a flow rate of 0.04 mL min^{-1} . A UV/Vis spectrometer was then used to measure the absorbance at 600 nm of the solution leaving the reactor and a graph was plotted of absorbance against time. This was repeated 4 times and an average residence time distribution was taken for each spacer. This was found by taking the points where the graph showed 50% absorbance at each side of the peak and the RTD was the time between these points.

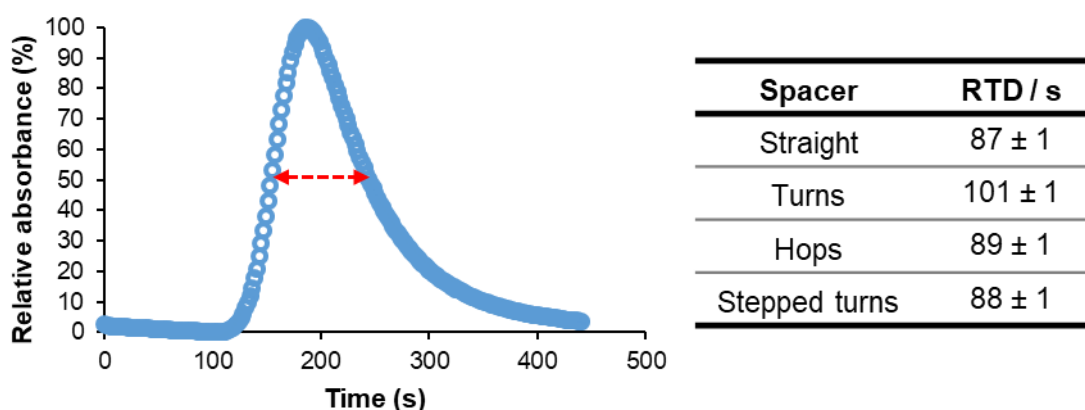


Figure S16: The residence time distribution was calculated as the time between 50% relative absorbance and the residence time distributions for the four spacers.

F, **H** and **I** all have the same RTD, suggesting that there is no back mixing. **G** has a longer RTD due to the shape of the flow channel. **G** has the same volume and electrode

surface area as the other spacers, however due to the meandering flow channel the outlet is only 40 mm away from the inlet. Consequently a straight channel 50 mm in length was needed to carry the solution to the outlet of the reactor. This channel was insulated from the electrodes and therefore should have no impact on the electrochemistry but it will increase the RTD because more diffusion can occur.

The axial dispersion coefficient (D_{ax}) was calculated using Equation S3,⁵ giving a good fit to the experimental curves when D_{ax} was $2.5 \times 10^{-4} \text{ m}^2 \text{ s}^{-1}$ (Figure S17).

$$E_t = \frac{u}{\sqrt{4\pi D_{ax}t}} \exp\left[-\frac{(L-ut)^2}{4D_{ax}t}\right]$$

Equation S3: Calculating the axial dispersion coefficient (D_{ax}). Where u is the average velocity, t is the time, L is the length and E_t is the exit time.

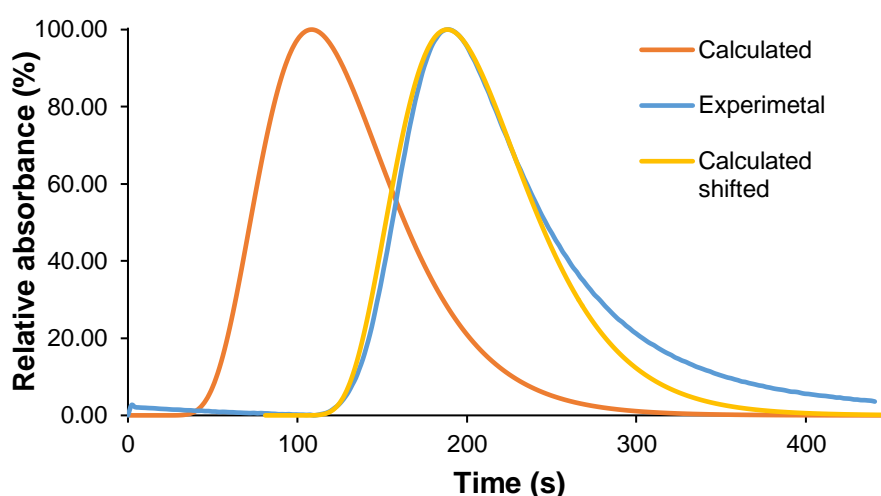


Figure S17: Experimental RTD with modelled RTD where $D_{ax} = 2.5 \times 10^{-4}$ and $N_L = 0.06$.

5.2.2. Mass transfer coefficients

Mass transfer coefficients can be calculated in electrochemical flow reactors by using the limiting current method. When an electrochemical reaction is taking place there is the transfer of electrons, which can be observed as a current. By increasing the potential the rate of the electrochemical step is increased and consequently the current. When the mass transfer of species to the electrode surface becomes the rate limiting step the current plateaus despite an increase in the potential. From this the mass transfer coefficient may be calculated. Finally, once the potential increases enough, solvent degradation results in the current increasing once again.

$$k_m = \frac{I_{lim}}{nFAC_B}$$

Equation S4: Calculating the mass transfer coefficient (k_m) from the limiting current (I_{lim}). Where n is the number of electrons exchanged, F is the Faraday constant and C_B is the concentration of the bulk solution.

A solution of potassium hexacyanoferrate (II) trihydrate (2.11 g, 5 mmol), potassium hexacyanoferrate (III) (3.29 g, 10 mmol) and sodium carbonate (5.30 g, 50 mmol) in water (100 mL) was prepared and pumped through a reactor with graphite electrodes at a flow rate of 0.04 mL min⁻¹. The current was recorded at increasing voltages and a graph of current against voltage was plotted to determine the limiting current of the spacer. These were then used to calculate the mass transfer coefficient for the spacers and could be compared to calculated values.

When scaling up the energy input (*via* pumping power due to pressure drop) is of considerable importance. The energy dispersion rate (EDR) was calculated from the pressure drop obtained through CFD, scaled to reflect the slightly shorter channel lengths. The mass transfer coefficients were then divided by the EDR, showing that hops offer an energy efficient means for increasing mass transfer.

Channel	Flow rate / m ³ s ⁻¹	P drop / Pa	EDR / W	km/EDR / m s ⁻¹ W ⁻¹
Straight	6.67E-10	2.5406	1.69E-09	1.15E+06
Turns	6.67E-10	2.5717	1.71E-09	1.01E+06
Steps	6.67E-10	2.8146	1.88E-09	1.40E+06
Hops	6.67E-10	2.8141	1.88E-09	3.23E+06

Table S17: Calculated energy dispersion rate (EDR) and ratio of km:EDR.

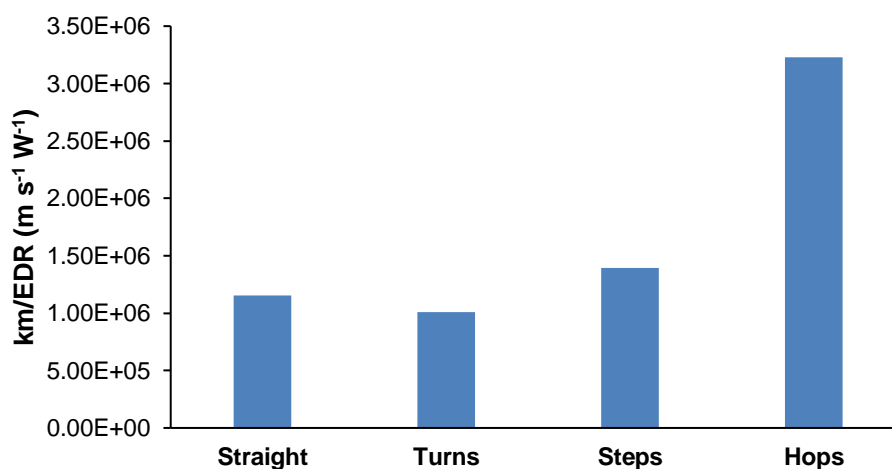


Figure S18: Ratio of mass transfer coefficient to energy dispersion rate for the different spacers.

5.2.2.1. Straight channel

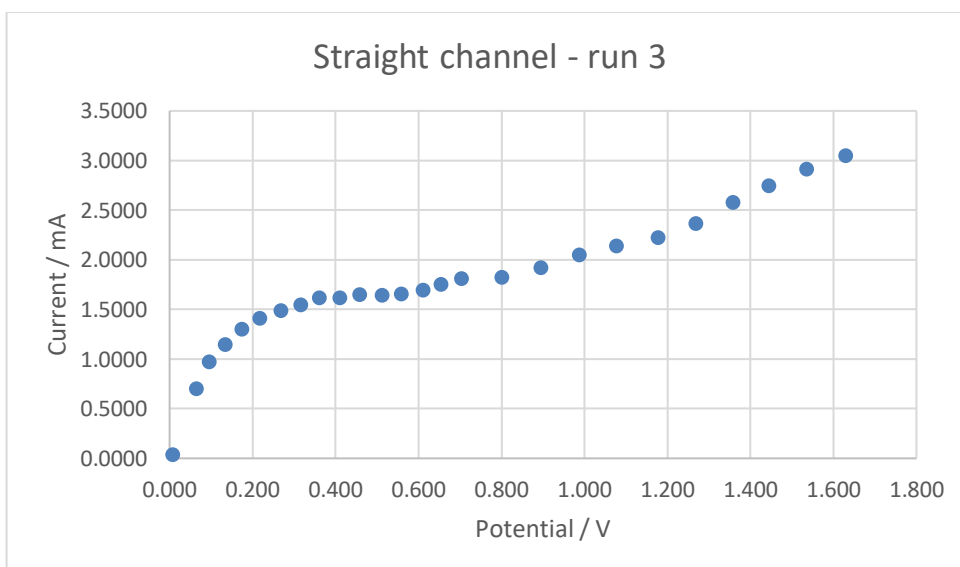
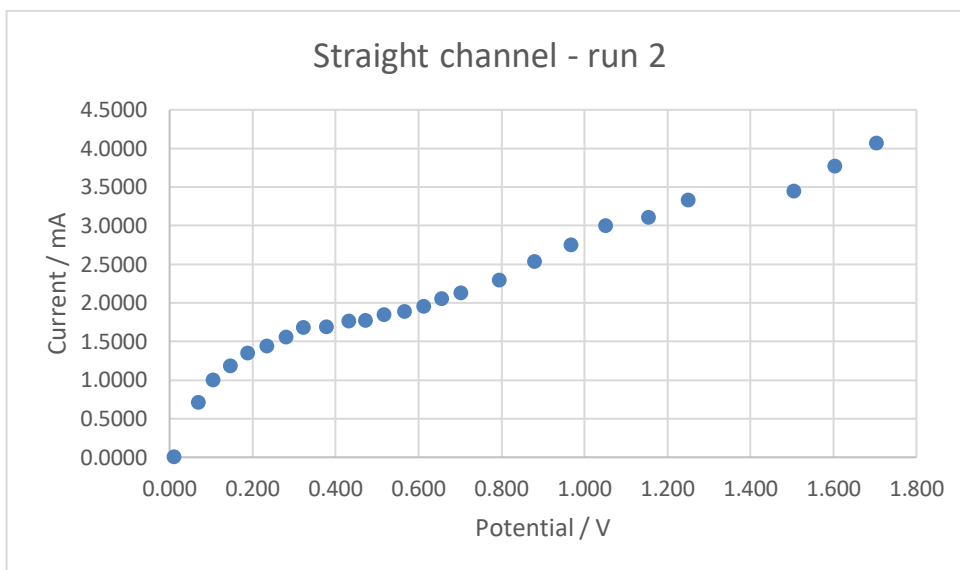
Run Number	Limiting Current / mA	km / m s ⁻¹
2	1.7682	0.00204
3	1.6138	0.00186
4	1.7038	0.00196
Average	1.6953	0.00195
Std Dev.	0.0776	0.00009

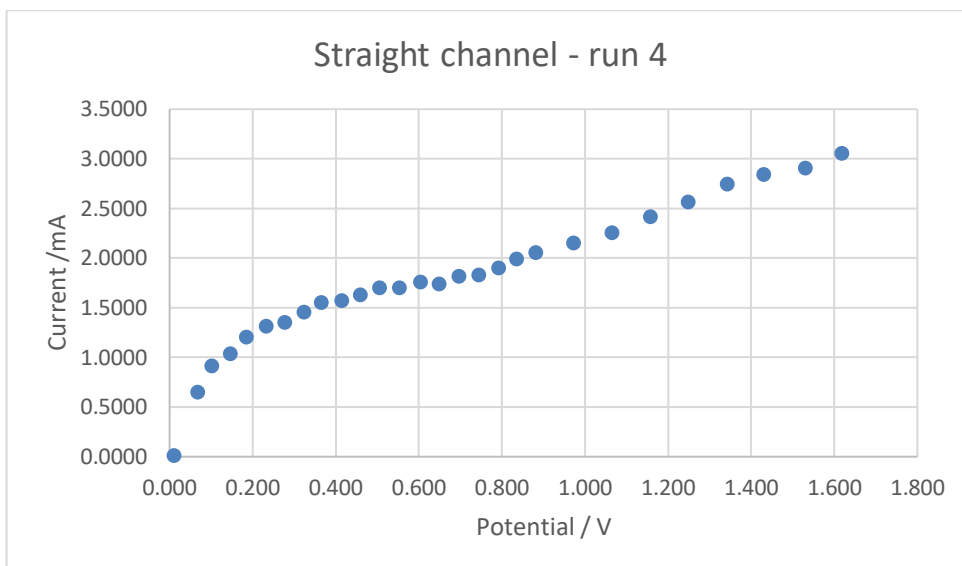
Std Error in mean

0.0448

0.00005

Table S18: Limiting current and calculated mass transfer coefficient for F.

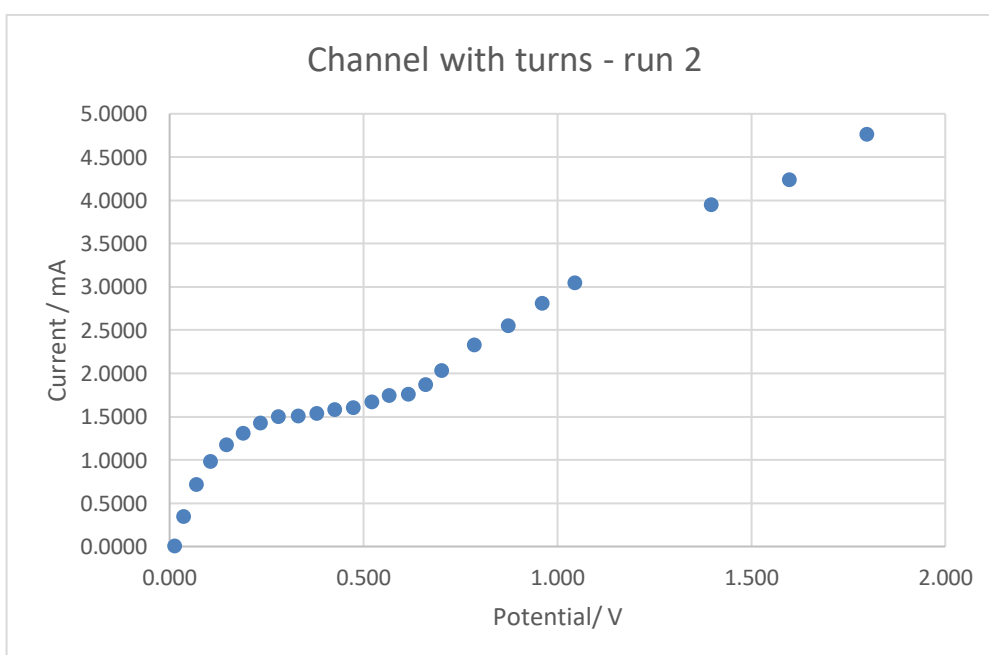


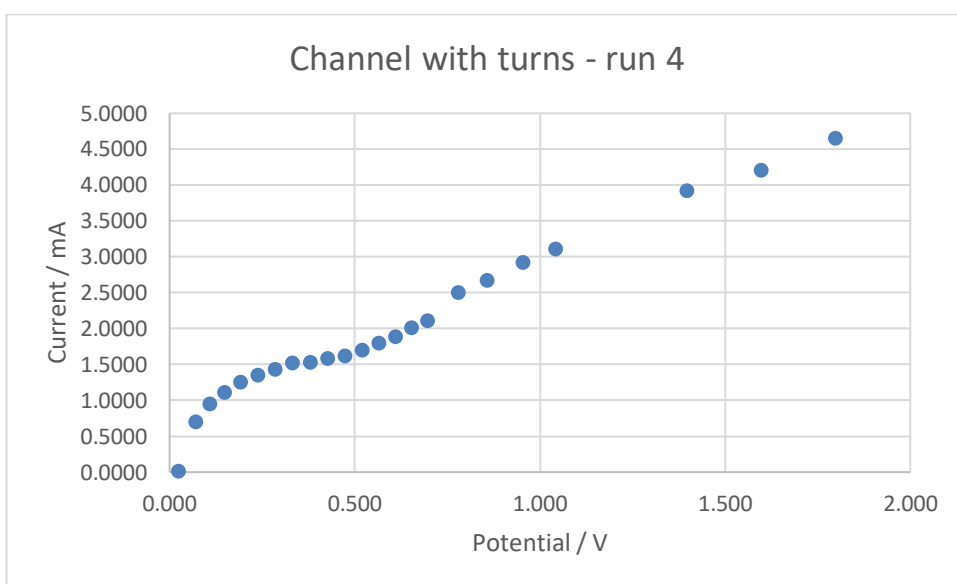
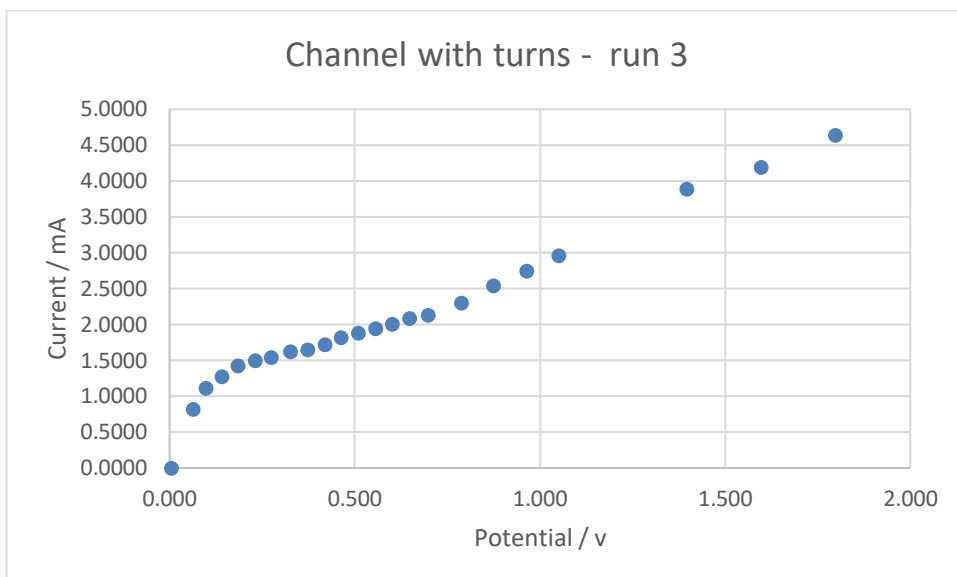


5.2.2.2. Channel with turns

Run No.	Limiting Current / mA	km
2	1.5000	0.00173
3	1.4996	0.00173
4	1.5140	0.00174
Average	1.5045	0.00173
Std. Dev.	0.0082	9.44394E-06
Std. Error in Mean	0.0047	5.45246E-06

Table S19: Limiting current and calculated mass transfer coefficient for **G**.

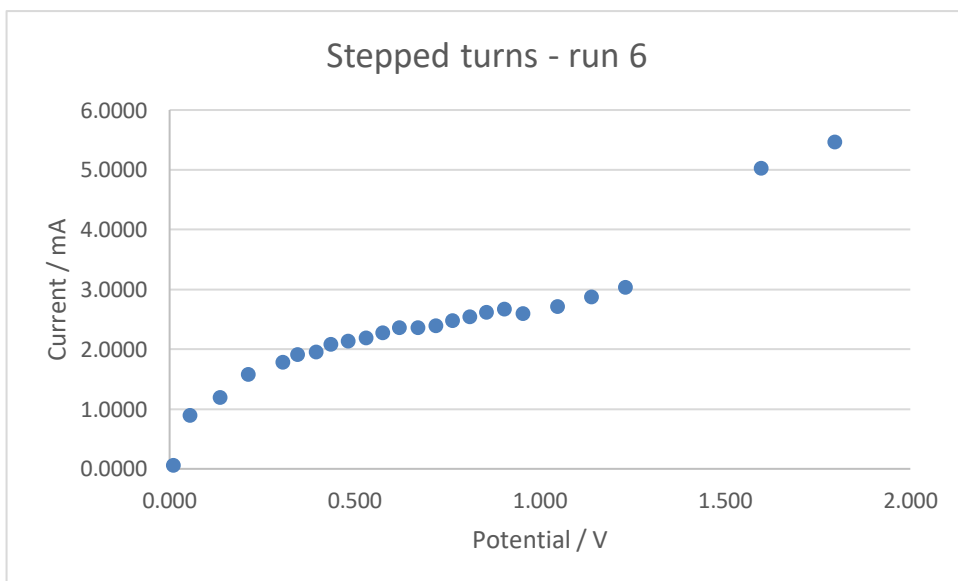
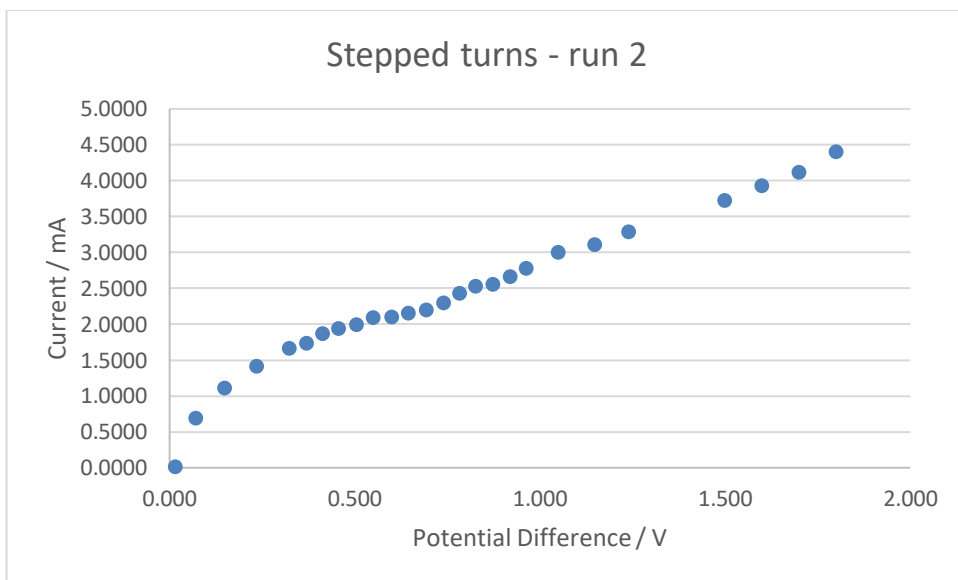
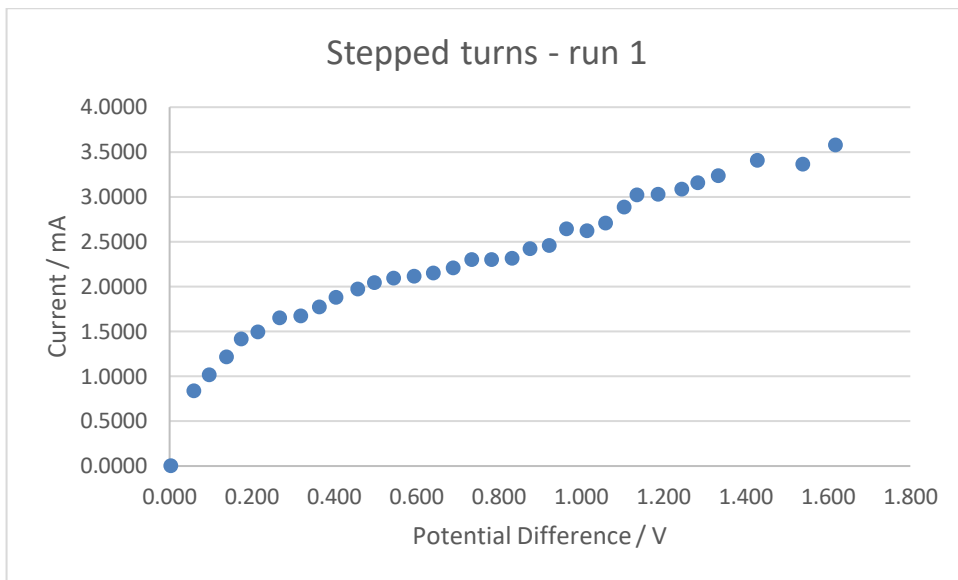


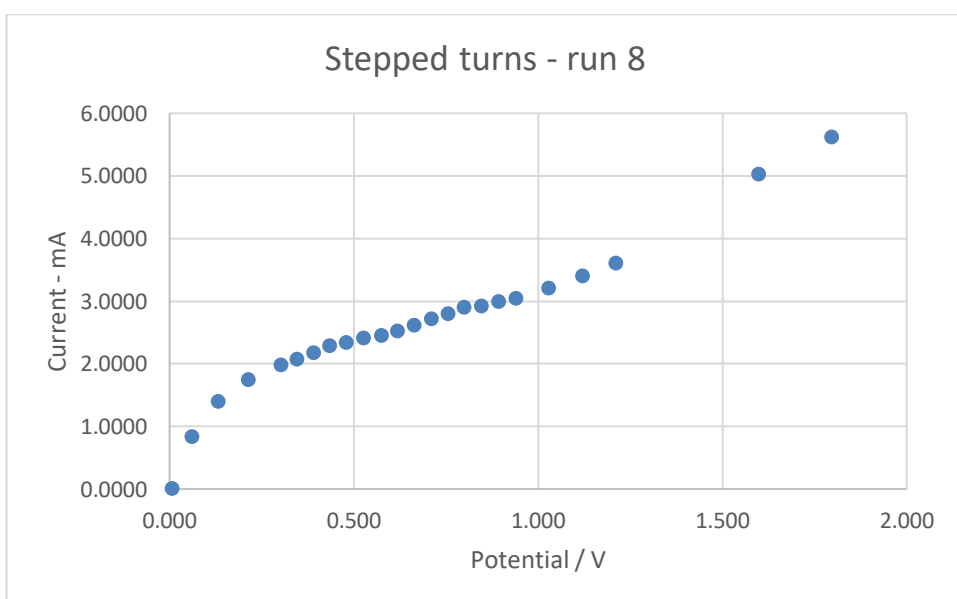
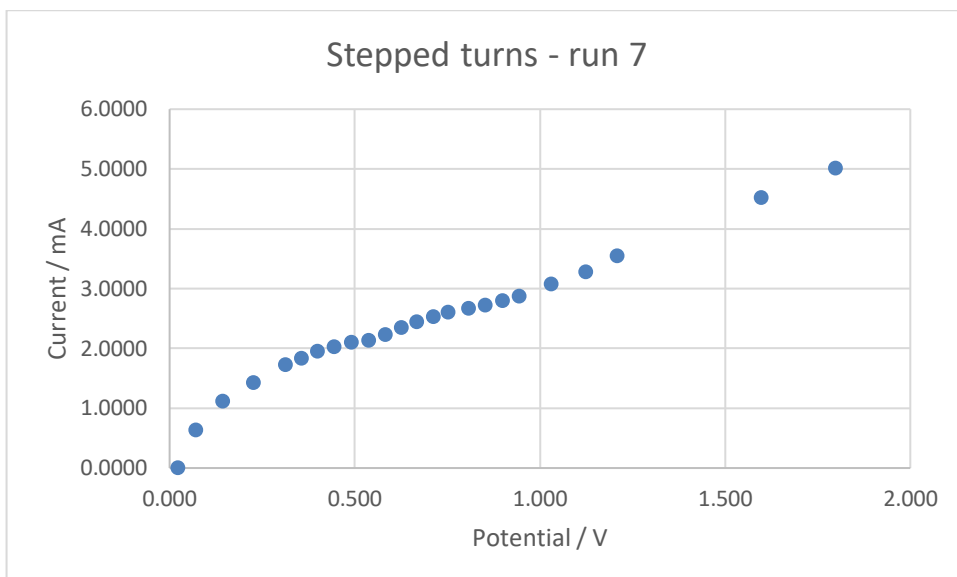


5.2.2.3. Channel with stepped turns

Run Number	Limiting Current / mA	km / m s ⁻¹
1	2.3064	0.00266
2	2.0986	0.00242
6	2.3610	0.00272
7	2.1428	0.00247
8	2.4516	0.00282
Average	2.2721	0.00262
Std. Dev.	0.1484	0.00017
Std. Error in Mean	0.0664	0.00008

Table S20: Limiting current and calculated mass transfer coefficient for H.

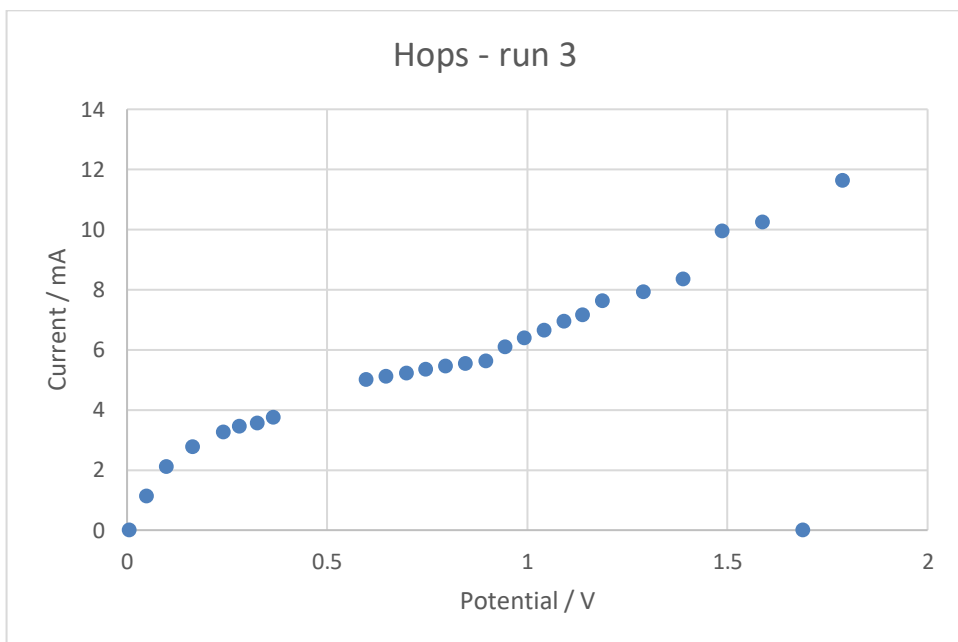
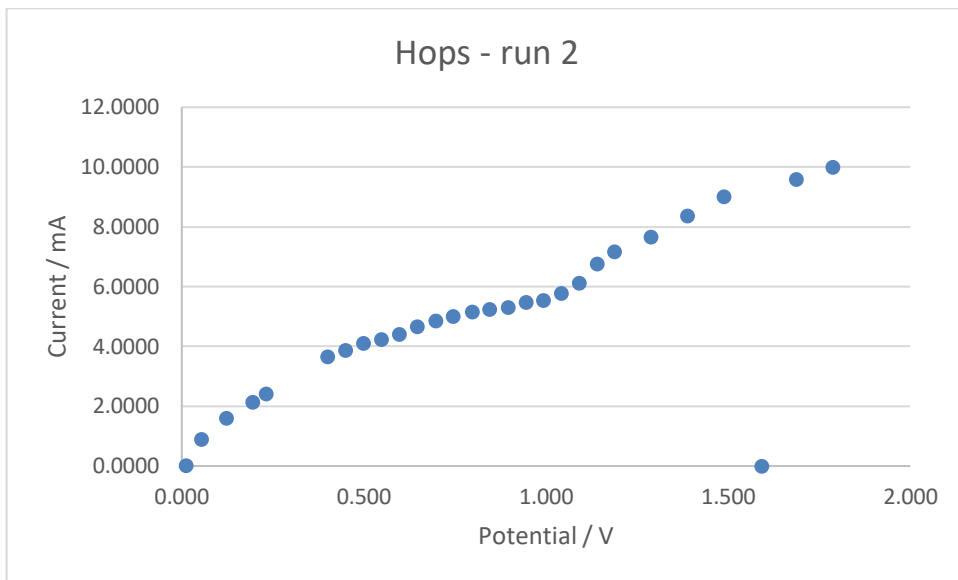


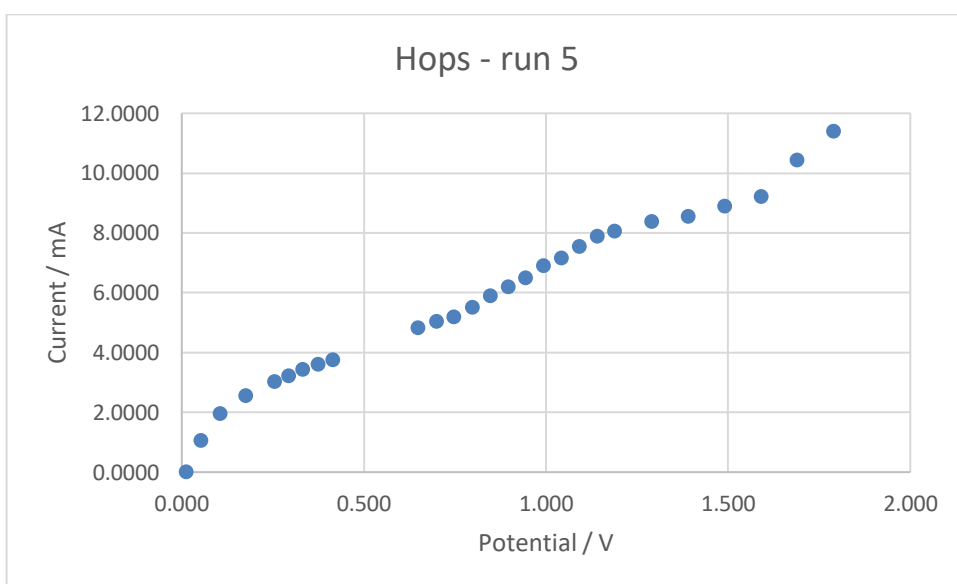
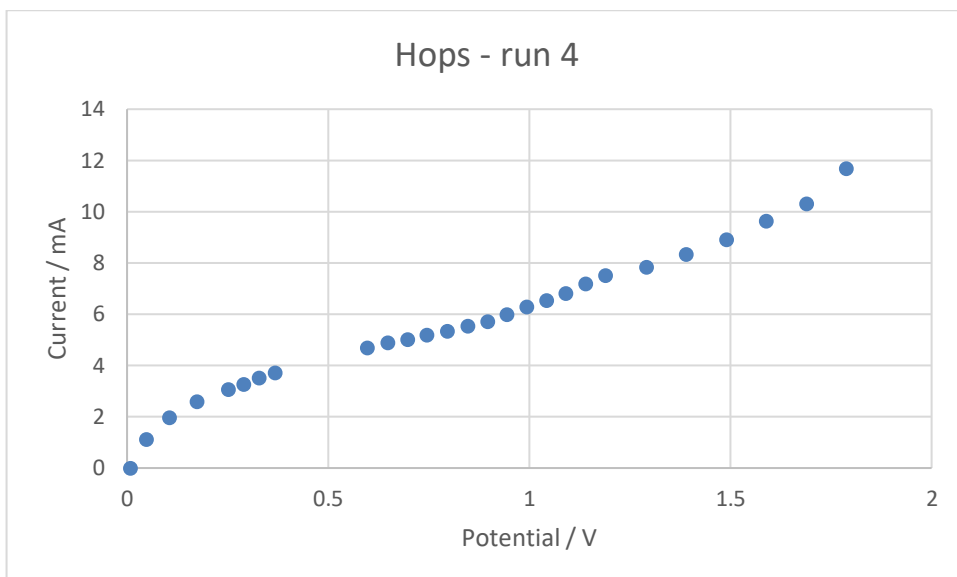


5.2.2.4. Channel with hops

Run No.	Limiting Current / mA	Km / m s ⁻¹
2	5.3000	0.00610
3	5.5400	0.00638
4	5.0200	0.00578
5	5.1800	0.00597
Average	5.2600	0.00606
Std. Dev.	0.2191	0.00025
Std. Error in Mean	0.1265	0.00013

Table S21: Limiting current and calculated mass transfer coefficient for I.





6. References

- 1 M. R. Chapman, Y. M. Shafi, N. Kapur, B. N. Nguyen and C. E. Willans, *Chem. Commun.*, 2015, **51**, 1282–1284.
- 2 C. Schotten, C. J. Taylor, R. A. Bourne, T. W. Chamberlain, B. N. Nguyen, N. Kapur and C. E. Willans, *React. Chem. Eng.*, 2021, **6**, 147–151.
- 3 H. R. Stephen, C. Schotten, T. P. Nicholls, M. Woodward, R. A. Bourne, N. Kapur and C. E. Willans, 0–5.
- 4 O. C. Zienkiewicz, R. L. Taylor and P. Nithiarasu, *The Finite Element Method for Fluid Dynamics*, Elsevier Butterworth Heinemann, Amsterdam, The Netherlands, 6th edn., 2005.

- 5 D. Rossi, L. Gargiulo, G. Valitov, A. Gavriilidis and L. Mazzei, *Chem. Eng. Res. Des.*, 2017, **120**, 159–170.